Role of the step curvature in the stabilization of coherently strained epitaxial structures

P Krapf, Y. Robach, Michel Gendry, L. Porte

Role of the step curvature in the stabilization of coherently strained epitaxial structures

P. Krapf and Y. Robach
Département de Physique-Chimie des Matériaux, UMR 5512, Ecole Centrale de Lyon, Boîte Postale 163, 69131, Ecully Cedex, France

M. Gendry
Laboratoire d'Electronique, Automatique, Mesures Electriques associé au CNRS, UMR 5512, Ecole Centrale de Lyon, Boîte Postale 163, 69131, Ecully Cedex, France

L. Porte*
Département de Physique-Chimie des Matériaux, UMR 5512, Ecole Centrale de Lyon, Boîte Postale 163, 69131, Ecully Cedex, France
(Received 12 December 1996)

Strained $In_{1-x}Ga_xAs$ epilayers have been grown on InP(001) by molecular-beam epitaxy both for 2% compressive strain ($x=0.18$) and 2% tensile strain ($x=0.75$). After an initial stage of layer-by-layer growth, coherent three-dimensional structures were observed by scanning tunneling microscopy in both cases. The shape of these three-dimensional structures is determined by elastic relaxation of the strained layers: while compressive strain favors convex step curvatures leading to three-dimensional islands, a tensile strain favors concave curvatures leading to three-dimensional holes. It is shown using a two-dimensional Laplace-Young relationship that a tensile-step specific stress stabilizes the step curvature. [S0163-1829(97)50416-4]

Interest in the epitaxial growth of lattice-mismatched semiconductors has increased since it appeared that it may be a method to make quantum dots: strains due to the mismatch can relax not only by dislocations, but also by the formation of coherently strained three-dimensional (3D) structures. This coherently strained Stranski-Krastanov growth has been observed in various systems: Ge on Si,[1,2] In(Ga)As on GaAs,[3–7] and $Ga_xIn_{1-x}P$ on InP.[8,9] A good understanding of the morphology is needed, since quantum-dot structures require self-organized islands with low size dispersion. Theoretical studies showed that island formation is due to the competition between strain relaxation and surface energy.[10] Relevant models for island shapes and sizes are available in several systems.[11,12] However macroscopic models often fail to describe atomic steps. Pseudomorphic epitaxial growth of $In_{1-x}Ga_xAs$ on InP can induce either compressive or tensile strain depending on the stoichiometry: compressive for $x<0.47$, tensile for $x>0.47$. Compressively strained indium-rich materials are of more interest for quantum dots since they have a narrower band gap than lattice-matched layers, while tensilely strained gallium-rich layers have a larger band gap. Therefore previous studies have principally focused on compressively strained layers. However, tensile layers are of interest in strain-compensated structures, where compressive and tensile layers are grown alternatively. Although little work has been done on tensile strain, it has been shown recently that the step energy depends on the sign of the strain,[13] and that it may influence the surface morphology.[14] In this paper we focus on the effect of the sign of the strain on surface morphology of $In_{1-x}Ga_xAs$ epilayers grown on InP. It is shown using the scanning tunneling microscope (STM), that compressive strain favors convex steps and then the formation of a 3D island morphology, while tensile strain favors concave steps, and then the formation of a 3D hole morphology.

$In_{1-x}Ga_xAs$ epilayers were grown by molecular-beam epitaxy on $n+InP(001)$ substrates. After thermal desorption of the native oxide of the substrate, a 400-nm-thick lattice-matched $In_{0.53}Ga_{0.47}As$ buffer layer was first grown on InP(001) in order to smooth the surface. This buffer layer was Si doped at 5×10^{18} atoms/cm^3, but the last 5 nm were kept undoped in order to avoid influence of the doping on the upper layer growth. 2% mismatched $In_{1-x}Ga_xAs$ layers were grown on this buffer layer, with a compressive strain for $x=0.18$, or a tensile strain for $x=0.75$. Growth was carried out under As stabilization with a V–III flux ratio of 80 at a relatively slow growth rate (0.25 μm per hour) and at high temperature (525 °C) in order to favor surface diffusion and obtain near-equilibrium shapes. For 2% mismatch this system exhibits a transition from a layer-by-layer growth mode to coherent island formation.[15,16] Reflection high-energy electron-diffraction (RHEED) patterns were registered during growth. For compressive strain, RHEED patterns showed the well-documented 2×4 surface reconstruction. The RHEED patterns became suddenly spotty at a critical thickness of 1.5 nm. This is characteristic of a two- to three-dimensional growth mode transition. For tensile strained layers a 2×1 surface reconstruction was observed by RHEED. However in that case the evolution of the diffraction pattern intensity was progressive, and no precise critical thickness could be determined from these observations. Several thicknesses were realized, ranging from 0.5 to 17 ML. After growth interruption, samples were quickly cooled to 300 °C, while arsenic pressure was maintained in order to reduce surface reorganization. Thereafter they were cooled to room temperature and transferred under vacuum into the contiguous STM chamber.[17] STM images were recorded at a sample bias of +2 V and with a tunneling current of 0.2 nA.

Step heights are a multiple of 0.3 nm, which is the distance between two As layers. In the following a monolayer

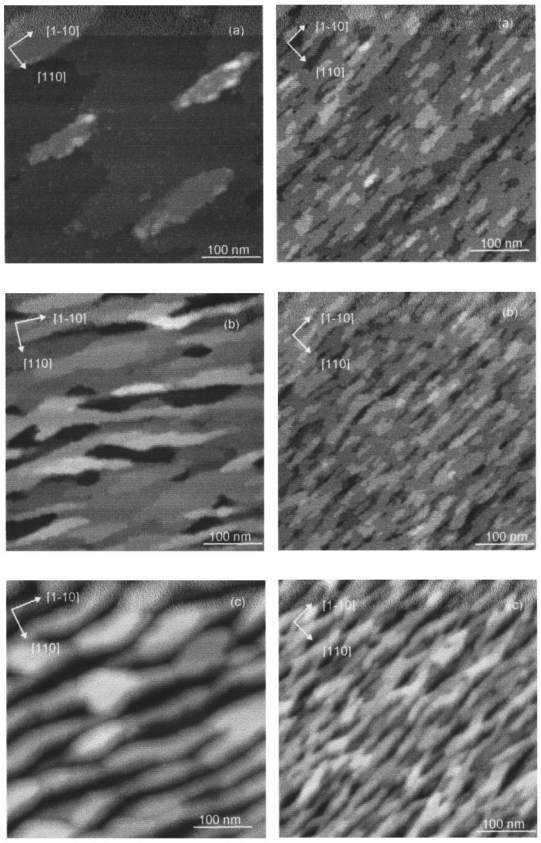

FIG. 1. STM images of epilayers grown on InP(001) for increasing thicknesses. The modification of the surface morphology with the deposit thickness shows the growth anisotropy and the evolution from layer-by-layer growth to three-dimensional growth: (A) Compressively strained layers ($x=0.18$, $\varepsilon=-2\%$). The 2D–3D growth mode transition is manifest between 4 and 5 ML: (a) Deposited thickness of 4 ML with localized 3-ML-high terraces. (b) Deposited thickness of 5 ML with 6–7-ML-high 3D platelets. (c) Deposited thickness of 10 ML with 15–20-ML-high islands. (B) Tensilely strained layers ($x=0.75$, $\varepsilon=+2\%$). 3D holes form progressively with deposited thickness. (a) Deposited thickness of 5 ML with 2-ML height variations. (b) Deposited thickness of 9 ML with 3-ML height variations. (c) Deposited thickness of 13 ML with 7-ML height variations.

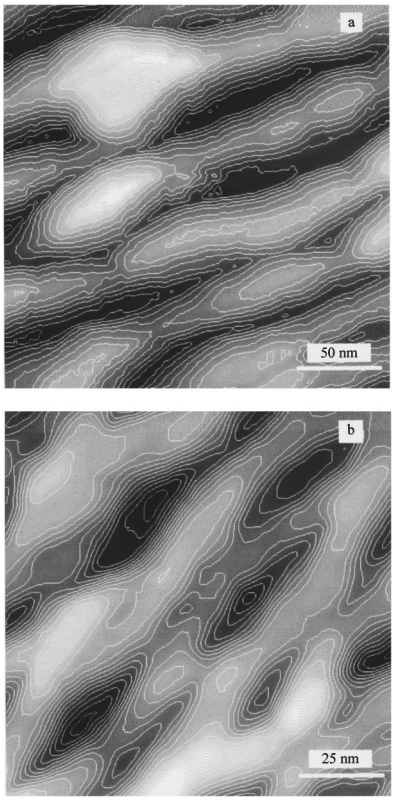

FIG. 2. STM images of the 3D structures. Images are presented in gray scale, so that deep areas appear dark, and high areas appear bright. Isohypses are drawn to emphasize that islands have grown in the case compression, while holes stay in the growing layer in the case tension (see text). (a) Deposit of a 10-ML compressive layer. White lines are isohypses 2 ML (6 Å) apart in height. (b) Deposit of a 13-ML tensile layer. White lines are isohypses 1 ML (3 Å) apart in height.

refers to a monomolecular layer of III and V elements. Beyond size measurements, the shape of the steps can help in understanding the roughening process. The convexity and concavity of a step can be defined with respect to the upper terrace position: if the upper terrace is inside (outside) the curvature, then the step is convex (concave). Thus a hole is concave and an island is convex. Figure 1 shows the evolution of surface morphology with a deposited thickness for a compressive strain [Fig. 1(a)] and a tensile strain [Fig. 1(b)]. As long as the growth remains two dimensional, only 1- or 2-, occasionally 3-ML-high terraces are observed on STM images for both signs of the strain. For a compressive strain almost all steps are convex, and are often more than 1 ML high (2 or 3 ML). For a tensile strain, both convex and concave steps are present. It can be noticed that the terrace nucleation process necessarily produces convex terraces both for compressive and tensile strains. Several thicknesses were realized with different last layer coverages. No influence on the shape of the steps was noticed. Thus near-equilibrium growth conditions are achieved and steps tend to have their equilibrium shape. For thicker deposits, three-dimensional anisotropic structures form for both tensile and compressive strains. While a critical thickness of 1.5 nm for the 2D–3D growth mode transition is observed for a compressive strain, the roughening is rather progressive for a tensile strain. In both cases platelets elongated along the [110] direction can be observed, while a height undulation is manifest in the [110] direction. This suggests that the strain is relaxed mainly along the [110] direction. 3D structures present size differences between tension and compression: the periodicity along [110] is about 30 nm for compression and 15 nm for tension. Figure 2 shows the 3D morphology of layers with compressive [Fig. 2(a)] and tensile [Fig. 2(b)] strain. A difference in the concavity of steps along [110] is also manifest. Steps running along [110] (i.e., steps perpendicular to the arsenic dimers) are called *B* steps, and steps running along [110] (i.e., steps parallel to the arsenic dimers) are called *A* steps. *A* steps are created during the 2D–3D growth mode transition, and participate in the relaxation of the strain along [110]. In the following we concentrate on *B* steps which are perpendicular to the direction in which strain is less relaxed. Statistics on the shape of the steps are obtained by scanning

the images with a line running along [110]. Each time the line is tangent to a step, the sign of the curvature (convex vs concave) was determined by the upper terrace position. A regular succession of isohypses has been drawn on Fig. 2 in order to identify the shape of the steps. For a compressive layer, 55% of the *B* steps are convex. Moison *et al.*[18] showed that a strong 2D–3D transition is due to movements of atoms from already complete layers. Figure 2 confirms that the development of islands (convex steps) is accompanied by hole creation (concave steps) besides the islands. The movement of atoms leads to a final morphology in which the difference between maxima and minima (7–8 ML) is higher than the average deposited thickness (5 ML). However, the main phenomenon is the formation of islands. For tensile layers, 70% of the *B* steps are concave. Thus the main features of the surface morphology of tensile strained layers can be described as holes rather than islands. On gray scale STM images, these holes appear as a negative replica of islands. Observations made at different growth stages indicate that tensile strain favors concave steps, while compressive strain favors convex steps.

In the following, we will analyze the stress relaxation which favors convex vs concave curvatures. A one-dimensional step stress can be defined, in the same way as the surface stress tensor,[19] by

$$\sigma^{1D}=\frac{1}{L}\frac{\partial E(\text{step})}{\partial \varepsilon} \tag{1}$$

where $E(\text{step})$ is the step energy, L the length of the step, and ε the one-dimensional strain. This one-dimensional step stress might be taken into account as a boundary condition to calculate the local stress field in the material. However an elementary analysis may explain qualitatively the influence of this 1D stress on the surface morphology. Figure 3(a) shows a curved *B* step. Call R the curvature radius of the step; dl the small step element tangent to [110] at one side, and making the angle α with [110] at the other side; and σ^{1D} the 1D stress which applies at the right end of the element dl. Forces along [110] compensate for two elements dl symmetric with respect to [110] while forces along [110] are summed. The projection of σ^{1D} along [110] equals $\sigma^{1D}\sin\alpha$ which gives at first order $\sigma^{1D}dl/R$. Thus a force per unit length equal to σ^{1D}/R has to be opposed normally to the step to maintain equilibrium. Stress in the upper layer can be analyzed as a 2D stress. The force applying on the step edge corresponds to the 2D stress difference $\Delta\sigma^{2D}$, which arises on both sides of a step [Fig. 3(b)]: 2D stress equals zero on the lower terrace side, and has a nonzero value due to bulk strain on the upper terrace side. Considering only stresses in the [110] direction, one can write

$$\Delta\sigma^{2D}=\sigma^{2D}(\text{external})-\sigma^{2D}(\text{internal}). \tag{2}$$

With $\sigma^{2D}(\text{external})=0$ and $\sigma^{2D}(\text{internal})<0$ in the case compression (island formation, upper terrace inside the curvature) and $\sigma^{2D}(\text{external})>0$ and $\sigma^{2D}(\text{internal})=0$ in the case tension (hole formation, upper terrace outside the curvature). Also,

$$\Delta\sigma^{2D}=\frac{\sigma^{1D}}{R}. \tag{3}$$

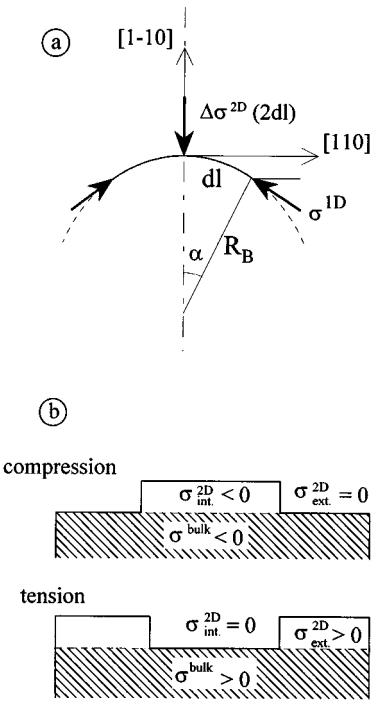

FIG. 3. (a) Representation of forces applying on a convex step edge for a compressively strained layer. The dl line elements have been drawn symmetric with respect to the [110] direction. The line tension equilibrates the 2D stress difference between both sides of the step (see text). (b) Origin of the 2D stress difference for a compressively strained platelet (island) and a tensilely strained incomplete terrace (hole).

It can be noted that this equation is a two-dimensional case of the well-known Laplace-Young relationship. At growth temperature steps are likely to move. They can be stable if forces applying on them compensate. Relation (2) shows that $\Delta\sigma^{2D}$ is always positive. Then according to relation (3), a positive (tensile) 1D stress, σ^{1D}, can stabilize both convex steps (islands) in the case compression and concave steps (holes) in the case tension. It can be inferred from the work by Xie *et al.*[13] that straight steps should sustain some tensile stress. While stress is well relaxed along [110] by the 3D morphology, it remains poorly relaxed along [110], since the surface does not present clearly identified height modulations in this direction. If a uniform strain field is assumed, the 2D stress difference between both sides of a step can be calculated from the bulk strain:

$$\Delta\sigma^{2D}=h\sigma^{3D}=\frac{hE}{(1-\nu)}\,\varepsilon\,, \tag{4}$$

where h is the height of one monomolecular step, and E and ν, respectively, the Young modulus and Poisson coefficient of $In_{1-x}Ga_xAs$. E and ν can be obtained by a linear interpolation of the values for InAs and GaAs.[20] The surface stress difference is then used to calculate the 1D step stress by introducing the experimentally observed curvature radii. These radii were evaluated graphically from STM images by drawing average curved steps describing the general oblong shape of islands and holes. For $x=0.18$ (compression) the radius is $R=15$ nm and using Eqs. (3) and (4) one obtains $\sigma^{1D}=8\times10^{-9}$ J/m (5 eV per Å). For $x=0.75$ (tension) the

radius is $R=5$ nm and one obtains $\sigma^{1D}=3\times10^{-9}$ J/m (1.9 eV per Å). According to Eq. (1), a tensile 1D stress implies that a compressive strain decreases the step energy, while a tensile strain increases it. Although the dependence of the 1D stress upon step curvature is not known, one can roughly estimate using Eq. (1) that a strain of 2% would lead to a variation of the step energy of the order of 150–400 meV per ledge atom. These results are obtained for two different alloy compositions corresponding to 2% tensile strain ($x=0.75$) and 2% compressive strain ($x=0.18$). They compare with the molecular-dynamics simulation of Xie *et al.*,[13] who obtained an energy variation of 150 meV per ledge atom for similar steps on 2% strained $Si_{0.5}Ge_{0.5}$ grown on relaxed buffers on a silicium substrate. The curvature of *B* steps is stabilized since it participates in stress relaxation. The approach proposed here may give a way to determine experimentally the stress of curved steps.

In conclusion of this epitaxial growth study on the $In_{1-x}Ga_xAs$ system, we have shown that compressively strained layers ($x=0.18$) grown on a buffer layer ($x=0.47$) lead to the formation of coherent 3D islands, while tensile strained layers ($x=0.75$) lead to the formation of 3D holes. The shape of islands and holes is determined by the steps of the small terraces which form these 3D structures. Steps from 3D islands adopt a general convex curvature, while steps from 3D holes adopt a general concave curvature. These results can be explained in the framework of a two-dimensional Laplace-Young relationship.

*Corresponding author; electronic address: louis.porte@cc.ec-lyon.fr

[1] D. J. Eaglesham and M. Cerullo, Phys. Rev. Lett. **64**, 1943 (1990).

[2] F. K. LeGoues, M. C. Reuter, J. Tersoff, M. Hammar, and R. M. Tromp, Phys. Rev. Lett. **73**, 300 (1994).

[3] C. W. Snyder, B. G. Orr, D. Kessler, and L. M. Sander, Phys. Rev. Lett. **66**, 3032 (1991).

[4] J. Massies and N. Grandjean, Phys. Rev. Lett. **71**, 1411 (1993).

[5] D. Leonard, M. Krishnamurthy, S. Fafard, J. L. Merz, and P. M. Petroff, J. Vac. Sci. Technol. B **12**, 1063 (1994); D. Leonard, M. Krishnamurthy, C. M. Reaves, S. P. Denbaars, and P. M. Petroff, Appl. Phys. Lett. **63**, 3203 (1993); D. Leonard, K. Pond, and P. M. Petroff, Phys. Rev. B **50**, 11 687 (1994).

[6] A. Madhukar, Q. Xie, P. Chen, and A. Konkar, Appl. Phys. Lett. **64**, 2727 (1994).

[7] J.-Y. Marzin, J.-M. Gerard, A. Israel, D. Barrier, and G. Bastard, Phys. Rev. Lett. **73**, 716 (1994).

[8] N. Carlsson, W. Seifert, A. Peterson, P. Castrilo, M. E. Pistol, and L. Samuelson, Appl. Phys. Lett. **65**, 3093 (1994).

[9] C. M. Reaves, V. Bressler-Hill, S. Varma, W. H. Weinberg, and S. P. Denbaars, Surf. Sci. **326**, 209 (1995).

[10] J. Tersoff, Phys. Rev. B **43**, 9377 (1991).

[11] J. Tersoff and R. M. Tromp, Phys. Rev. Lett. **70**, 2782 (1993).

[12] C. Priester and M. Lannoo, Phys. Rev. Lett. **75**, 93 (1995).

[13] Y. H. Xie, G. H. Gilmer, C. Roland, P. J. Silverman, S. K. Buratto, J. Y. Cheng, E. A. Fitzgerald, A. R. Kortan, S. Schuppler, M. A. Marcus, and P. H. Citrin, Phys. Rev. Lett. **73**, 3006 (1994).

[14] D. E. Jones, J. P. Pelz, Y. H. Xie, P. J. Silverman, and G. H. Gilmer, Phys. Rev. Lett. **75**, 1570 (1995).

[15] M. Gendry, V. Drouot, C. Santinelli, G. Hollinger, C. Miossi, and M. Pitaval, J. Vac. Sci. Technol. B **10**, 1829 (1992).

[16] L. Porte, P. Krapf, Y. Robach, M. Phaner, M. Gendry, and G. Hollinger, Surf. Sci. **352-354**, 60 (1996).

[17] P. Krapf, J. P. Lainé, Y. Robach, and L. Porte, J. Phys. (France) III **5**, 1871 (1995).

[18] J. M. Moison, F. Houzay, F. Barthe, L. Leprince, E. André, and O. Vatel, Appl. Phys. Lett. **64**, 196 (1994).

[19] R. C. Cammarata, Prog. Surf. Sci. **46**, 1 (1994).

[20] A. D. Prins and D. J. Dustan, in *Properties of Lattice-Matched and Strained InGaAs*, edited by P. Bhattacharya (INSPEC, London, 1993), p. 43.